Core-excited $Ar^*(2p_{3/2}{}^{-1}\ nl)$ atoms inside an Ar crystal: Effect of Ar neighbors on the excited state

J. P. Gauyacq
Laboratoire des Collisions Atomiques et Moléculaires, Unité Mixte de Recherche CNRS-Université Paris Sud UMR 8625, Bâtiment 351, Université Paris-Sud, 91405 Orsay Cedex, France
(Received 23 November 2004; published 31 March 2005)

The modifications induced on the core-excited $Ar^*(2p_{3/2}{}^{-1}\ 4s)$ state by Ar neighbors inside solid Ar are studied via a microscopic model of the system associated to a wave-packet propagation treatment of the excited electron. Different environments, built up from finite size pieces of an fcc Ar crystal are considered. The Ar neighbors are shown to influence the excited 4*s* electron energy both via confinement of the excited orbital and via polarization of the surrounding medium. The difference between the 4*s* orbital and higher lying excited orbitals is stressed by considering the wave function of various excited orbitals inside a bulk environment. The present results are compared with available experimental results on the $Ar^*(2p_{3/2}{}^{-1}\ 4s)$ state inside and at the surface of solid Ar.

DOI: 10.1103/PhysRevB.71.115433 PACS number(s): 78.70.Dm, 71.35.−y, 73.20.Hb, 77.55.+f

I. INTRODUCTION

When an atom (a molecule) is embedded in a host medium or adsorbed on the surface of a host medium, its electronic properties can be strongly affected by the interaction with its environment. In particular, excited electronic states that can spread over a rather large volume in space can be much sensitive to their surroundings. The influence of environment is, for example, revealed when considering transient excited states at surfaces and their role in surface reaction mechanisms.[1,2] Furthermore, depending on the site on the surface or inside the solid, one can expect different modifications of the excited state and then different dynamical behaviors in reactive mechanisms. An appealing model system for analyzing environment effects on the excited state energy is provided by core-excited atoms inside an insulator environment, such as the $Ar^*(2p_{3/2}{}^{-1}\ 4s)$ state inside solid Ar which is studied here. In such a system, the localized character of the core excitation severely limits the traveling possibility of the excitation during the excited state lifetime, so that the excitation can be considered as localized on one site of the crystal, then allowing for the analysis of site-dependent effects. Secondly, although the excitation energy of the system is large, the excited electron cannot decay by transfer of the excited electron into the solid conduction band; such core-excited states only decay by multielectron interactions. As a consequence, the analysis of the $Ar^*(2p_{3/2}{}^{-1}\ 4s)$ state energy can be performed easily and reveals the influence of the solid environment on the 4*s* excited orbital.

The core-excited $Ar^*(2p_{3/2}{}^{-1}\ 4s)$ state in an Ar solid environment has been the subject of several experimental studies in the past years.[3–7] In the case of $Ar^*(2p_{3/2}{}^{-1}\ 4s)$ atoms embedded inside bulk Ar, the excitation energy of the $Ar^*(2p_{3/2}{}^{-1}\ 4s)$ state from the ground state was found to be shifted by a significant amount (0.7–1.0 eV) from its value in the free atom.[8,9] This effect of the environment on the excited state energy was attributed to the confinement of the 4*s* orbital by the Ar neighbors in the crystal (also called "caging" effect). The 4*s* electron energy is inside the Ar crystal band gap. The Ar neighbors repel the excited electron, which cannot expand freely in space leading to an increase of its kinetic energy. A similar effect has also been observed in the case of $Ar^*(2p_{3/2}{}^{-1}\ 4s)$ atoms located at the surface of an Ar solid, however, with a smaller shift of the excitation energy.[3,5–7] Recently, core-excited $Ar^*(2p_{3/2}{}^{-1}\ 4s)$ atoms have also been studied experimentally in the case of Ar clusters and the excitation energy has been measured as a function of the cluster size for both $Ar^*(2p_{3/2}{}^{-1}\ 4s)$ atoms located inside the cluster or on its surface.[10,11] These measurements clearly showed the effect of the environment on the excited state energy, which appears to vary with the site (on the cluster surface or inside the cluster) and with the cluster size. For completeness, one can also mention experimental studies of the $Ar^*(2p_{3/2}{}^{-1}\ 4s)$ state in the case of Ar atoms adsorbed on metal surfaces or inside atomically thin Ar layers adsorbed on metal surfaces.[4,7,12–14] In this case too, the environment (metal+Ar) of the excited state was found to significantly alter the excited state properties. However, on a metal surface, the dynamics of the excited state is deeply modified by the coupling with the metal conduction band that brings a new decay channel for the excited state via transfer of the excited electron into the metal. This system presents strong site effects: both the energy of the excited state and the dynamics of the electron transfer into the metal were found to strongly depend on the Ar^* location in the system.

The aim of the present theoretical work is to determine how the Ar neighbors inside an Ar crystal modify the energy of the excited state. This is performed via the study of the $Ar^*(2p_{3/2}{}^{-1}\ 4s)$ state inside a few different environments. This problem has already been studied using a spherical model of the Ar surroundings,[15] in which the perturbation of the Ar neighbors is modeled by an additional potential, spherically symmetric around the Ar center; in this case,[15] only global absorption spectra summing up the contributions from all the various atoms in given icosahedra clusters have been reported (see also Ref. 16 for a review on atomic spec-

tra perturbations inside spherical cages). In the present work, we use a microscopic representation of the Ar atoms surrounding the core-excited state, allowing a detailed analysis of the environment effect. For this purpose, we study the $Ar^*(2p_{3/2}{}^{-1}\ 4s)$ atom inside a finite size piece of an Ar fcc crystal. Varying the size and geometry of the system allows an analysis of the energy of the excited state as a function of the number of Ar neighbors. This study is performed with the microscopic model description of solid Ar developed to study the effect of thin Ar films on image potential states[17,18] and also applied to a study of the $Ar^*(2p_{3/2}{}^{-1}\ 4s)$ state in a thin Ar film adsorbed on a metal surface.[19] In the latter case, it was possible to show how the neighboring Ar atoms and metal surface influence the excited state properties. Two main effects were invoked: confinement and polarization of the excited orbital; both effects are shown below to play an important role in the present study of finite size Ar crystals. At this point, it must be stressed that the present finite size objects are designed to illustrate the effects of Ar neighbors on the excited state energy in a solid environment and they cannot be considered as realistic Ar clusters although the corresponding results give some insight into the cluster case. A realistic cluster study would involve objects with well-defined size and structure, which, *a priori*, are not always pieces of a perfect fcc crystal.

II. METHOD

The system formed by a core-excited $Ar^*(2p_{3/2}{}^{-1}\ 4s)$ atom inside an Ar crystal has been studied using the same method as the one used in our earlier study of the $Ar^*(2p_{3/2}{}^{-1}\ 4s)$ atom adsorbed on a metal and of the electron transfer between the excited atom and the metal surface;[19] it makes use of a wave-packet propagation (WPP) method.[20] Only a brief overview is given here. The method consists in studying the time evolution of the outer 4*s* electron of the $Ar^*(2p_{3/2}{}^{-1}\ 4s)$ state by a one-electron WPP method. The environment of the $Ar^*(2p_{3/2}{}^{-1}\ 4s)$ atom is formed by a piece of an fcc Ar crystal with an Ar-Ar distance equal to that in bulk Ar, i.e., $d_{\text{Ar-Ar}}=7.03a_0$.[21] Calculations were performed using different numbers of Ar neighbors, up to a few hundreds (see below).

The Hamiltonian governing the evolution of the 4*s* electron is written as

$$H = T + V_{e\text{-Ar}^+\text{core}} + V_{e\text{-Ar crystal}}, \tag{1}$$

where T is the electron kinetic energy.

$V_{e\text{-Ar}^+\text{core}}$ is the excited electron interaction with the $Ar^+(2p_{3/2}{}^{-1})$ core. It is a pseudopotential of the Kleinman-Bylander[22] form. Its explicit expression is given in Ref. 19, where it has been adjusted to reproduce the binding energies of the outer *nl* electron in the $Ar^*(2p_{3/2}{}^{-1}\ nl)$ states as they are known from experiments on free Ar atoms.[8,9]

$V_{e\text{-Ar crystal}}$ is the interaction of the electron with the piece of Ar solid surrounding the core-excited Ar^*. The $V_{e\text{-Ar crystal}}$ potential is built from a model local potential $V_{e\text{-Ar}}$, describing the interaction between an electron and a single Ar atom; it is the sum of a short-range part and a long-range polarization part, and has been adjusted in Ref. 18 to describe the low-energy electron-Ar scattering. The electron-interaction between the electron and the finite size Ar crystal is obtained by the superposition of the interactions between the electron and the various Ar atoms in the crystal, with proper care of the polarization of each Ar atom by the electron, by the Ar^+ ion core and by the other polarized Ar atoms (see Ref. 18 for details). For the present study, we chose the definition of the $V_{e\text{-Ar crystal}}$ potential such as when the electron goes to infinity, the potential goes to the polarization energy of the Ar crystal by the remaining Ar^+ core. The present procedure for computing the $V_{e\text{-Ar crystal}}$ potential, taking the mutual polarization of the Ar atoms into account, ensures the proper dielectric character of the Ar crystal. It was found to be very accurate in describing low energy electrons inside bulk Ar as well as the perturbation induced by an atomically thin Ar layer on the Cu(100) image potential states.[18]

The electron wave packet $\Psi(\vec{r},t)$ is written in cylindrical coordinates (ρ,ϕ,z), with the z axis along a high symmetry axis of the fcc crystal. Depending on the number of Ar atoms and on the geometry of the piece of crystal that was considered, the z axis is a n-fold symmetry axis with $n=2$, 3, 4, or 6. Typically the grid involves ($n_\rho=400$, $n_\phi=64$, $n_z=256$) points. The points are equally spaced in ϕ and z coordinates, whereas coordinate mapping is used for the ρ coordinate (see Refs. 19 and 20 for details). The time propagation of the electron wave packet $\Psi(\vec{r},t)$, detailed in Ref. 19, is performed using the so-called "split" approximation.[23,24] The typical propagation time step is 0.1 a.u.

The propagation was started at time $t=0$ with the wave packet $\Psi(\vec{r},0)$ equal to $\Phi_0(\vec{r})$, the 4*s* electron wave function in the free $Ar^*(2p_{3/2}{}^{-1}\ 4s)$ atom [for the tests calculations on other $Ar^*(2p_{3/2}{}^{-1}\ nl)$ core-excited states, the corresponding free atomic states were taken as initial states]. From the time-dependent wave packet $\Psi(\vec{r},t)$, one defines the survival amplitude of the system in the initial state

$$A(t) = \langle \Phi_0 | \Psi(\vec{r},t) \rangle. \tag{2}$$

The real part of the Laplace transform of $A(t)$ yields the density of states (DOS) of the system, projected on the initial state, i.e., on the 4*s* orbital of the free atom. Large peaks in the DOS as a function of the energy indicate the positions of the states with a large overlap with the atomic free 4*s* orbital (see Ref. 20 for details). In the present one-electron study in a finite system, the 4*s* electron has a negative energy with respect to vacuum and so, is in a stable bound state (the core hole decays via multielectron interactions not taken into account in the present study). In the projected DOS obtained with finite time propagation, the 4*s* state then appears as a peak with a finite width determined by the propagation time.

The wave function of the 4*s* electron has been computed with the method outlined in Ref. 20; it is obtained via the Laplace transform of the time-dependent wave packet $\Psi(\vec{r},t)$ at the state energy. If we assume that the shift of the $Ar^*(2p_{3/2}{}^{-1}\ 4s)$ absorption line due to the presence of the Ar crystal is only due to the change of the 4*s* one electron energy and to polarization energy,[19] the absorption line energy in the crystal case $E_{\text{abs}}^{\text{crystal}}$ can be approximated by

$$E_{\mathrm{abs}}^{\mathrm{crystal}} \approx E_{\mathrm{abs}}^{\mathrm{atom}} - E_{4s}^{\mathrm{atom}} + E_{4s}^{\mathrm{crystal}} - E_{\mathrm{pol}}, \tag{3}$$

where $E_{\mathrm{abs}}^{\mathrm{atom}}$ is the absorption line energy in the free atom case, E_{4s}^{atom} is the one electron energy of the 4*s* electron in the free atom (with respect to vacuum), $E_{4s}^{\mathrm{crystal}}$ is the one electron energy of the 4*s* electron in the crystal (with respect to vacuum and a crystal polarized by the Ar^+ core), and E_{pol} is the polarization energy of the Ar crystal by the Ar^+ ion core alone. With the present definition of the $V_{e\text{-Ar crystal}}$ potential (see above), the WPP calculation provides the energy of the outer 4*s* electron with respect to vacuum and an unpolarized finite size Ar crystal, i.e., the quantity $(E_{4s}^{\mathrm{crystal}} - E_{\mathrm{pol}})$. So comparing the 4*s* electron energy in WPP calculations with and without the Ar crystal surrounding the core-excited Ar^* directly yields the energy shift of the $Ar^*(2p_{3/2}{}^{-1}\,4s)$ absorption line, as given by Eq. (3). Equation (3) only considers changes in the 4*s* electron and polarization energies; as discussed below these changes correspond to the effect of the excited electron confinement and of electrostatic polarization interactions. These energy changes are thought to be stronger than the variation of the other interactions, in particular of the van der Waals interaction responsible for the Ar-Ar interaction in the ground state. Indeed, as shown below, the energy change for an Ar^* in bulk Ar is of the order of 0.9 eV, whereas the cohesive energy per atom in solid Ar is of the order of 80 meV. Equation (3) should then give a reasonable estimate of the Ar^* absorption line shift.

III. RESULTS

A. Energy shift of the $Ar^*(2p_{3/2}{}^{-1}\,4s)$ state as a function of its environment

We have determined the change in the 4*s* electron energy for a set of systems, in which the core-excited Ar^* is surrounded by a finite size fcc Ar crystal with a variable number of Ar neighbors. Both the number of nearest neighbors and that of more distant neighbors have been varied. For computer time saving, systems with a reasonably high symmetry have been favored; they were chosen such that a high symmetry rotation axis existed, that could be taken as the *z* axis in the WPP calculation.

The left panel of Fig. 1 summarizes the computed 4*s* energy shift as a function of the number of Ar first neighbors. Systems, in which only first neighbors are present around the core-excited Ar^* atom, are represented by filled circles, while systems with a certain number of additional more distant neighbors are represented by crosses. Some of the systems, in which only first neighbors are present around the core-excited Ar^* atom, are schematically depicted in Fig. 2. The simple systems only involving first neighbors correspond to (increasing number of first neighbors): a diatom, a triangle, a planar triangle surrounding Ar^* [schema (a) in Fig. 2], the (100) plane of the fcc crystal [schema (b) in Fig 2], the (111) plane [schema (c) in Fig. 3], the (100) surface [schema (d) in Fig. 2], the (111) surface [schema (e) in Fig. 2], bulk fcc with two vacancies, bulk fcc with one vacancy, and bulk fcc. For the systems corresponding to a plane, a surface or bulk Ar, the calculations with a variable number of distant neighbors involved larger systems, while keeping the nature and the symmetry of the simple object.

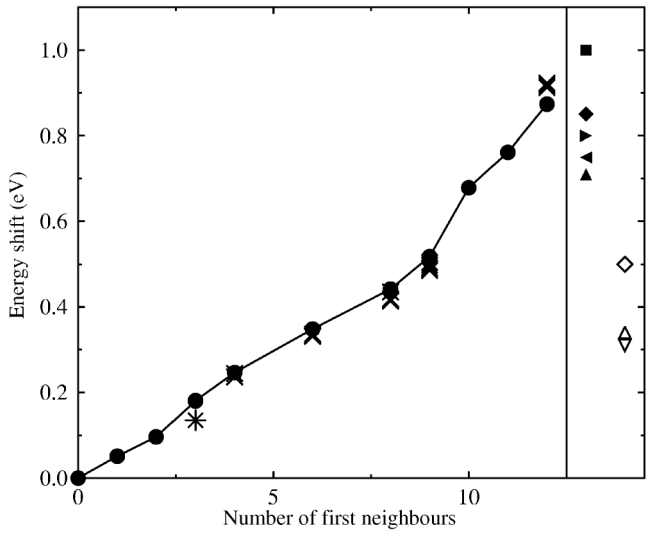

FIG. 1. Left panel: energy shift of the 4*s* excited electron in various environments, as a function of the number of nearest neighbors (see text for the definition of the various environments). Full circles: systems with only nearest neighbors. Crosses: systems with a variable number of distant neighbors. The star (three nearest neighbors) gives the result for Ar^* located at one of the corners of a tetrahedron. Right panel: experimental results for the energy shift of the $Ar^*(2p_{3/2}{}^{-1}\,4s)$ state in bulk Ar (full symbols) and on the surface of bulk Ar (open symbols). Bulk Ar: full square (Refs. 4–6), full diamond and right triangle (Ref. 3), full left triangle (Refs. 10 and 11), full up triangle (Ref. 7). Surface: open diamonds (Refs. 5 and 6), open up triangle (Ref. 11), open down triangle (Refs. 7 and 10).

As the first remarkable feature in Fig. 1, the energy shift of the 4*s* electron is seen to mainly depend on the number of first neighbors, the addition of second or larger order neighbors only slightly modifies the 4*s* energy shift. This aspect is further illustrated in Fig. 3, which presents an enlarged picture of the 4*s* energy shift for systems with nine first neighbors [(111) surface of the fcc] as a function of the total number of Ar neighbors. The largest system involved 284 Ar atoms. The convergence of the 4*s* energy is detailed for two kinds of systems: a system formed by only a 2 ML thin film or by a thicker film. The Ar distant neighbors located both close to the surface or deep in the solid contribute to the energy shift. The convergence of the energy with the total number of Ar atoms is not very fast. However, the total energy shift due to the distant neighbors is small; in this case, it amounts to 30–40 meV, i.e., of the order of 7% of the total energy shift induced by all the neighbors.

The weak effect of the distant Ar neighbors corresponds to the localized character of the 4*s* orbital that is well concentrated around the excited atom (see below). The interaction with the distant Ar atoms is due to the anisotropic charge distribution around the Ar^* which polarizes the surrounding Ar medium. In the present case [(111) surface], the leading term corresponds to the dipole moment of the 4*s* orbital. It must be stressed that the convergence illustrated in Fig. 3 is much faster than the one for the polarization energy (E_{pol}),

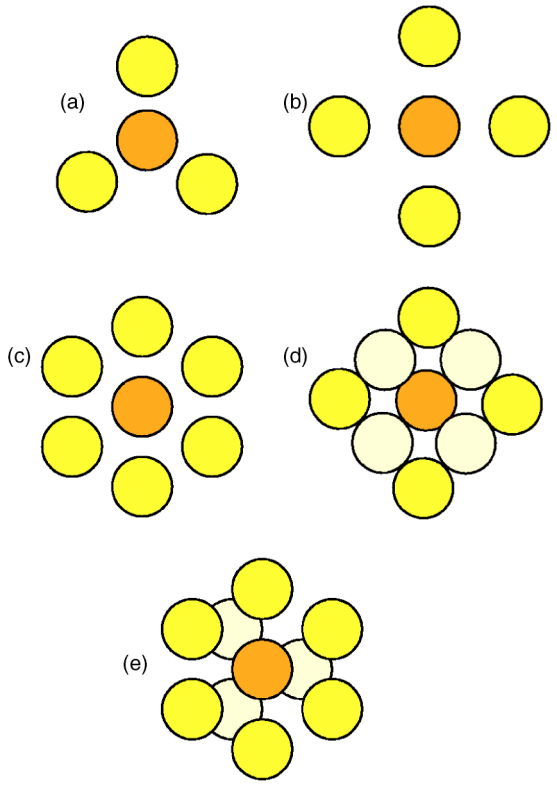

FIG. 2. (Color online) Schematic representation (top view) of some of the systems studied in the present work. The excited Ar^* atom is surrounded by some of its first neighbors in an fcc crystal. The excited Ar^* atom is symbolized by an orange sphere, the Ar first neighbors located in the same horizontal plane as Ar^* by yellow spheres, and the Ar first neighbors located in the second layer by light yellow spheres.

which involves the polarization of the Ar medium by a charge (see, e.g., the calculation of the change of the $2p_{3/2}$ energy in Ref. 25).

As a second remarkable feature of the results in Fig. 1, the energy shift roughly varies linearly with the number of first neighbors. The above features are quite consistent with the interpretation of the energy shift as being due to the confinement of the 4*s* orbitals by the Ar neighbors: confinement increases with the number of first neighbors; second and further neighbors do not significantly contribute to the confinement. This view is, however, too simple: one can notice that (i) the linear variation of the energy shift with the number of nearest neighbors is only approximate and (ii) distant neighbors appear to contribute in different ways to the energy shift, their effect being opposite for bulk Ar as compared to the case of planes and surfaces. One can also stress that the energy shift strongly depends on the geometry and symmetry of the object as illustrated in the case of three first neighbors. The energy shift is different for a planar object (Ar^* surrounded by a triangle) and a tetrahedron (Ar^* is one of the tetrahedron corners). The confinement of the 4*s* orbital can be thought to be different in the two cases. This difference can also be linked to the difference between surface and bulk systems discussed below.

All the results presented in Figs. 1 and 3 have been obtained for finite size fcc crystals with the Ar-Ar distance

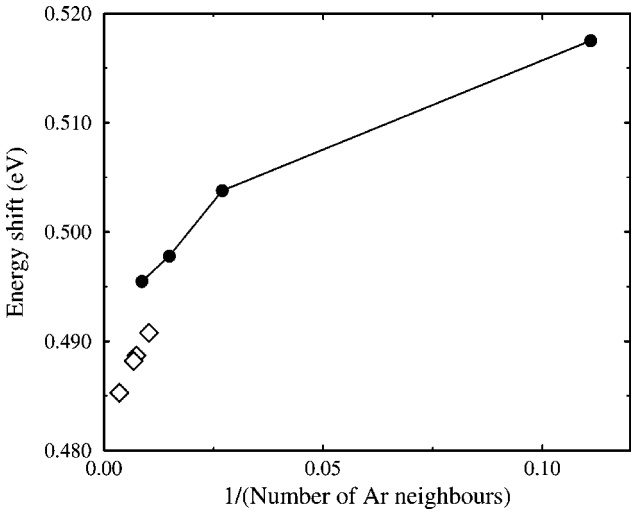

FIG. 3. Energy shift of the 4*s* excited electron in various environments as a function of the inverse of the total number of Ar atoms in the system. The Ar^* core-excited atom is surrounded by nine nearest neighbors following the geometry of the (111) surface of an fcc Ar crystal. Full circles: system formed by two atomic planes of variable size. Open diamonds: system formed by a layer of variable thickness (more than two atomic planes) and size.

equal to that of bulk Ar. However, one can expect the nearest-neighbor distance in a finite size system to differ from that in bulk Ar (see, e.g., the case of a thin atomic film on Cu in Ref. 18). To illustrate a possible effect of the Ar-Ar distance, Fig. 4 presents the result for the energy shift in the case of the system with only nine first neighbors [symmetry of a (111) surface, schema (e) in Fig. 2] as a function of the Ar-Ar distance. As expected for a confinement effect, the energy shift quickly increases when the Ar-Ar distance decreases. This can lead to significant effects when consid-

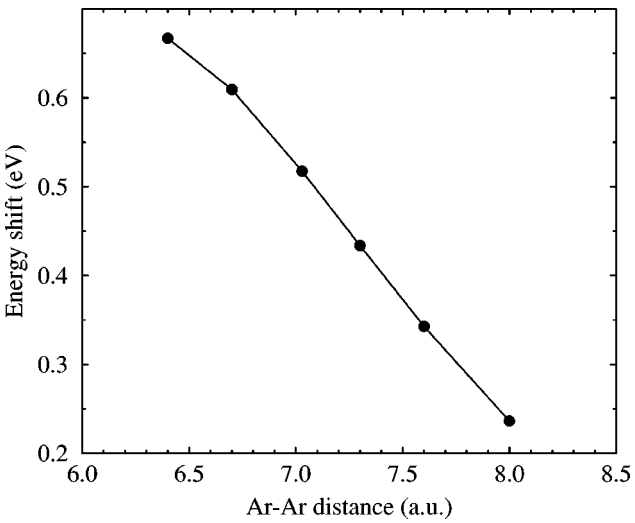

FIG. 4. Energy shift of the 4*s* excited electron as a function of the distance between two Ar neighbors. The Ar^* core-excited atom is surrounded by nine nearest neighbors following the geometry of the (111) surface of an fcc Ar crystal [schema (e) in Fig. 2]. The 4*s* energy shift is presented as a function of the distance between the Ar atoms.

ering finite size systems and/or adsorbed systems. As an example, 1 ML Ar adsorbs on Cu(100) with an Ar-Ar distance around $7.52a_0$ (Ref. 18) in contrast with the bulk distance of $7.03a_0$. In this system, the Ar adsorption is influenced by the structure of the Cu substrate, leading to an Ar-Ar distance quite different from that in bulk Ar. As seen in Fig. 4, such an Ar-Ar distance change would correspond to a 30% change of the energy shift in the systems considered here.

The opposite effects of the distant neighbors seen in Fig. 1 are surprising at first sight. In a pure confinement interpretation, one would expect the energy to increase with the number of neighbors, the effect rapidly decreasing with the distance. This feature is interpreted as a consequence of the polarization of the Ar medium by the 4*s* electron. Indeed, in a surface geometry, the 4*s* orbital is embedded in an anisotropic environment, allowing a mixture of *p* and *s* orbitals. The 4*s* orbital is then polarized and the associated dipole interacts with all the Ar atoms in the system, lowering the 4*s* energy shift. This interaction concerns both first and more distant neighbors and converges more slowly with the total number of neighbors than the confinement effect. This polarization of the 4*s* orbital is analogous to that found in the case of Ar atoms adsorbed on a metal surface,[19] although significantly weaker. In contrast, when the core-excited Ar^* atom is inside bulk Ar, the environment symmetry is O_h and symmetric and antisymmetric states with respect to the Ar^* center cannot mix. No dipole is present on the Ar^* which would polarize the surrounding medium (higher order multipoles are indeed possible). One can then expect the confinement to dominate with a 4*s* energy shift increasing with the number of neighbors. The different geometry of the surface and bulk environment leads to different physical situations and thus to different behaviors. This interpretation can also be used for the discussion of the nonexactly linear variation of the energy shift with the number of first neighbors, which exhibits a faster increase between 9 and 12 first neighbors (see Fig. 1). This can be linked to the change of geometry of the object: either a surface environment with a half free space where the 4*s* orbital can be polarized, or bulk surrounding without free space for the 4*s* electron to spread. The change of polarization energies between the two kinds of geometry could account for the steep rise of the energy shift between 9 and 12 neighbors. This interpretation can be further tested by looking at the wave functions of the 4*s* orbital in different environments.

B. Wave function of the 4*s* excited orbital in various environments

Figure 5 presents the wave function of the 4*s* orbital when the $Ar^*(2p_{3/2}{}^{-1}\ 4s)$ atom belongs to the (111) surface of an Ar solid. The Ar^* is surrounded by nine first neighbors and the calculation included a total number of 284 Ar atoms. The *z* axis of the WPP calculation is normal to the (111) surface and $z>0$ is in vacuum. The Ar^* is at the origin of coordinates. The calculation is three dimensional and the figure presents a cut of the 3D electron density in the $(11\bar{2})$ plane perpendicular to the surface, including the *z* axis and one of the axes parallel to the surface. One recognizes the 4*s* orbital

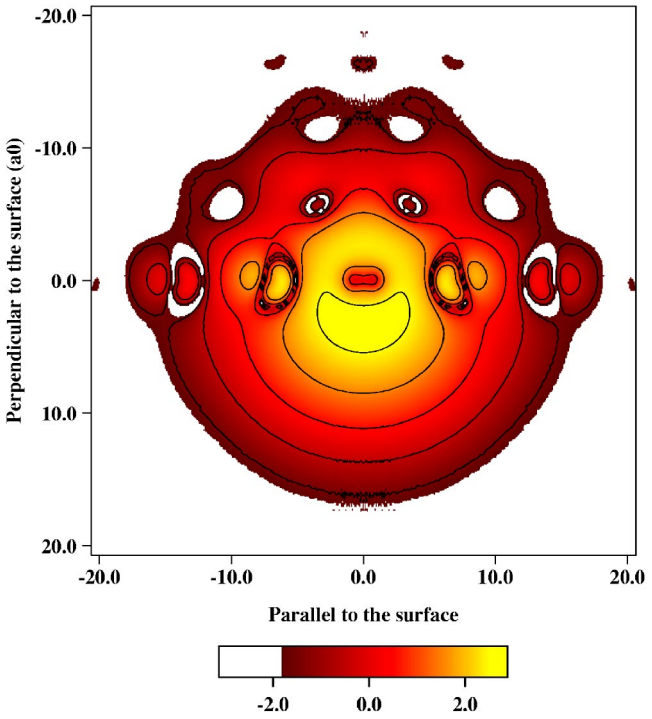

FIG. 5. (Color online) Contour plot of the resonant 4*s* orbital of a core-excited $Ar^*(2p_{3/2}{}^{-1}\ 4s)$ atom on the (111) surface of an fcc Ar crystal. The excited Ar^* atom is one of the surface atoms. The figure presents a cut of the logarithm of the modulus of the 4*s* electron wave function in the $(11\bar{2})$ plane normal to the surface in cylindrical coordinates parallel and perpendicular to the surface. The coordinate normal to the surface is positive in vacuum and the Ar^* atom center is located at the origin of coordinates. The electron density decreases when going from yellow to orange and deep red (from light to dark gray). White corresponds to very small electron densities. The contour lines (thin full lines) correspond to 1.0 steps.

described with a pseudopotential in the region around the origin of coordinates. In the free atom, it is a nodeless spherical orbital, very small around the atom center. The electronic cloud is significantly distorted from its spherical shape in the free atom, its maximum being outside of the crystal. Typically, the electron density maximum is shifted by $3a_0$ from the Ar^* center. However, despite this asymmetry, the 4*s* orbital main lobe is mainly located in the vicinity of the Ar^* center, and only the tail of the orbital spreads over a few Ar-Ar distances. The 4*s* electron energy lies inside the band gap of solid Ar and so the Ar crystal is a classically forbidden region for the 4*s* electron. Two nearest Ar neighbors on the surface appear as double lobe structures in the wave function. The shape of these structures is due to the orthogonality condition imposed by the *e*-Ar interaction potential. Since this potential binds two core levels (*s* and *p* symmetry in the free atom), the outer 4*s* orbital has to be orthogonal to these core levels. One can notice that the double lobe structure in the case of the nearest neighbors does not point toward the center of Ar^*. Its direction is rather determined by the distorted shape of the electronic cloud around the Ar^* and the double lobe structure points to the maximum of the 4*s* electronic cloud. The $(11\bar{2})$ plane of the figure only contains

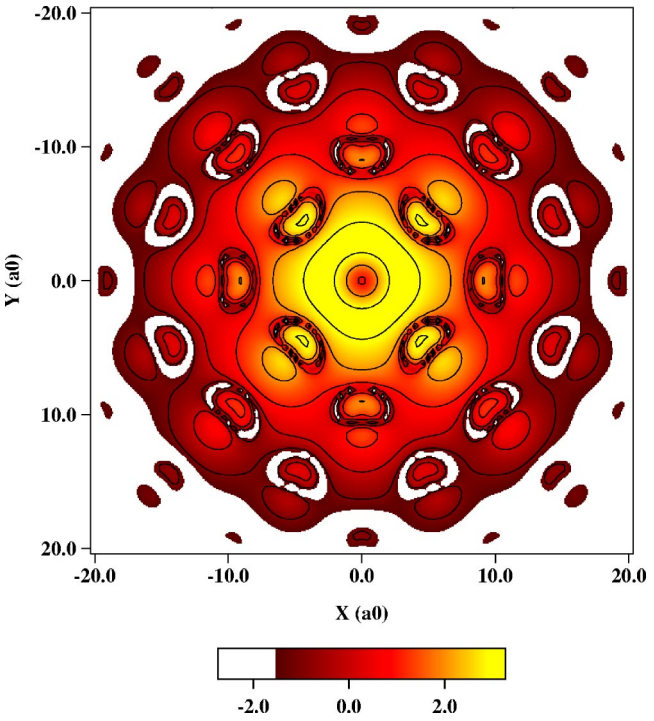

FIG. 6. (Color online) Contour plot of the resonant 4*s* orbital of a core-excited $Ar^*(2p_{3/2}{}^{-1}\ 4s)$ atom inside an fcc Ar crystal. The figure presents a cut of the logarithm of the modulus of the 4*s* electron wave function in the (100) plane (*x* and *y* coordinates). The Ar^* atom center is located at the origin of coordinates. The electron density decreases when going from yellow to orange and deep red (from light to dark gray). White corresponds to very small electron densities. The contour lines (thin full lines) correspond to 1.0 steps.

Ar atoms in the first layer and in the fourth layer. As a consequence, the orthogonality constraints due to the Ar atoms in the second and third layer are not very well marked since the corresponding atoms are not in the plane of the figure. The double lobe structure of the atom in the fourth layer is barely visible due to the distance from the Ar^* center. To summarize, the 4*s* orbital appears to be repelled by the nearest Ar neighbors that prevent the orbital to spread freely in the crystal and the orbital appears to be pushed into vacuum. There is thus a significant dipole associated with the 4*s* electronic cloud that can polarize the neighboring Ar crystal. The polarization of the 4*s* orbital appears similar to that found in the case of Ar^* adsorbed on a metal surface or on a thin Ar layer on a metal surface,[19] however, in a weaker manner.

The situation appears different in the case of the $Ar^*(2p_{3/2}{}^{-1}\ 4s)$ atom embedded inside bulk Ar, shown in Fig. 6. The Ar^* is at the center of the figure which presents a cut of the 4*s* wave function in the (100) plan. The ordinate axis is the *z* axis of the WPP calculation and is along the [001] direction of the Ar crystal. The calculation involved 381 Ar atoms. One recognizes the 4*s* electronic cloud around the origin of coordinates. It is strongly distorted by the four nearest neighbors present in the plane of the figure, which lead to the four strong double lobe structures surrounding the Ar^* center. Although distorted, the 4*s* electronic cloud remains mainly localized around the Ar^* center and does not spread much over the Ar crystal. Here again, the 4*s* electron is inside the band gap of solid Ar and cannot propagate into the Ar crystal. The 4*s* orbital exhibits the symmetry of its environment, it is symmetric with respect to the origin and thus is not associated with an electric dipole. Figures 5 and 6 then fully confirm the interpretation of a 4*s* orbital confined by its Ar neighbors and prevented from spreading into the Ar crystal. They also confirm the existence of a significant polarization of the electronic cloud in the case of a nonsymmetric environment. At this point, one can stress that, within the microscopic view analyzed here, the effect of the surrounding Ar medium appears as the nearest Ar atoms repelling the excited electronic cloud and confining it, whereas, within a continuous medium picture, one would discuss in terms of the 4*s* electron energy being inside the Ar band gap and thus of the 4*s* electron unable to propagate freely inside bulk Ar and associated with an evanescent wave inside the bulk.

C. Wave function of higher lying excited orbitals inside bulk Ar

The case of the $Ar^*(2p_{3/2}{}^{-1}\ 4s)$ state studied here corresponds to an excited orbital confined by its neighbors. The effect is particularly conspicuous, the size of the orbital being comparable to the distance to the nearest neighbor in bulk Ar. One can wonder about the case of an $Ar^*(2p_{3/2}{}^{-1}\ nl)$ core-excited state, in which the size of the corresponding excited orbital in the free atom is larger than the distance between Ar atoms in bulk Ar. Then, would the confinement picture still be valid or would the excited orbital spread over the crystal? To get some insight into this problem, we studied with the same method a few higher lying core-excited $Ar^*(2p_{3/2}{}^{-1}\ nl)$ states in bulk Ar.

Figure 7 presents a cut of the 5*s* orbital wave function for an $Ar^*(2p_{3/2}{}^{-1}\ 5s)$ atom embedded inside bulk Ar. The plane of the cut is the same as in Fig. 6, as well as the finite size of the Ar crystal (381 atoms). One recognizes the 5*s* orbital centered at the origin of coordinates. With the pseudopotential used here, the 5*s* orbital exhibits one node, which appears at a distance of about $4.5a_0$ from the center. The main lobe of the wave function is now spread over a large area of the crystal. It retains an overall spherical symmetry with localized structures around the Ar neighbors. The four nearest neighbors are associated with stronger structures, but distant Ar atoms also generate well-marked orthogonality structures. In Fig. 7, the 5*s* orbital does not look at all similar to an orbital confined by its neighbors but more similar to an orbital spread over the crystal and locally perturbed by the Ar centers. Since the orbital is large in space, discussing the effect of the Ar medium in terms of electrostatics inside a continuous medium is well adapted. In a continuous medium approach, the 5*s* orbital would be associated to a spherical evanescent wave inside the Ar. As for the energy, if one considers a system formed by a unit positive charge inside a medium of dielectric constant ε ($\varepsilon_{Ar}=1.7$ for solid Ar), the binding energy of a given state varies as ε^{-2}. In the present case of a 5*s* orbital, the binding energy in the free atom[8,9] is equal to 1.709 eV. For the $Ar^*(2p_{3/2}{}^{-1}\ 5s)$ atom inside the Ar crystal, the binding energy is equal to $(-E_{4s}^{\text{crystal}}+\Delta V)$, where ΔV is the position of the bottom of the conduction band in Ar

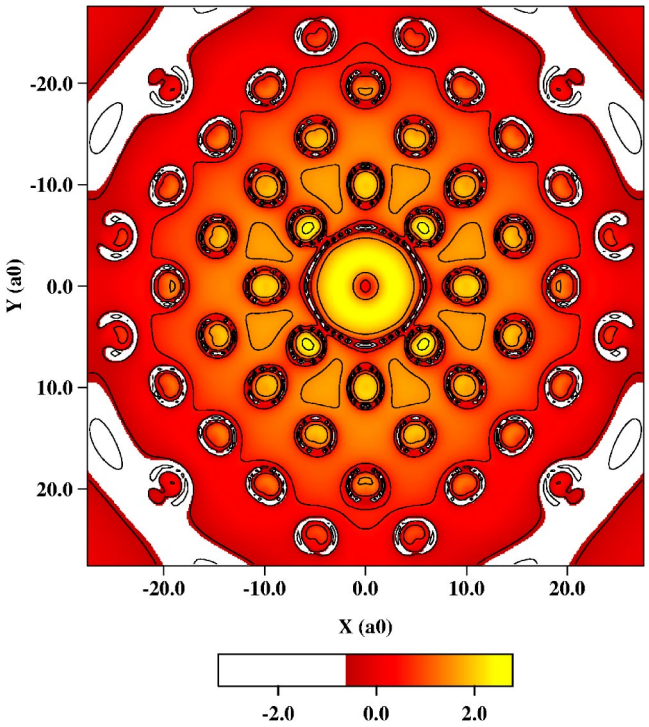

FIG. 7. (Color online) Contour plot of the resonant 5*s* orbital of a core-excited $Ar^*(2p_{3/2}^{-1}\,5s)$ atom inside an fcc Ar crystal. The figure presents a cut of the logarithm of the modulus of the 5*s* electron wave function in the (100) plane (*x* and *y* coordinates). The Ar^* atom center is located at the origin of coordinates. The electron density decreases when going from yellow to orange and deep red (from light to dark gray). White corresponds to very small electron densities. The contour lines (thin full lines) correspond to 1.0 steps.

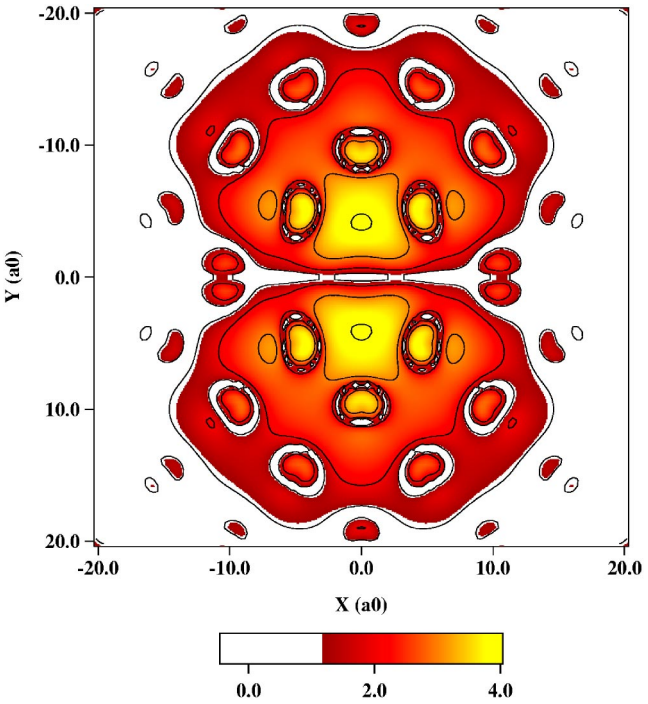

FIG. 8. (Color online) Contour plot of the resonant 4*p* orbital of a core-excited $Ar^*(2p_{3/2}^{-1}\,4p)$ atom inside an fcc Ar crystal. The figure presents a cut of the logarithm of the modulus of the 4*p* electron wave function in the (100) plane (*x* and *y* coordinates). The Ar* atom center is located at the origin of coordinates. The electron density decreases when going from yellow to orange and deep red (from light to dark gray). White corresponds to very small electron densities. The contour lines (thin full lines) correspond to 1.0 steps.

with respect to vacuum [$\Delta V = 0.23$ eV in the present modeling of solid Ar (Ref. 18)]. The 5*s* binding energy in the medium is equal to 0.76 eV, i.e., a change of the binding energy by a factor $(1.5)^{-2}$, consistent with the $\varepsilon_{\mathrm{Ar}}^{-2} = (1.7)^{-2}$ factor. In addition to the approximations implied by the continuous medium approach, the difference between the two values can be attributed to the nonpure Coulombic nature of the e-Ar^+ core interaction. One can also mention that the 5*s* binding energy in the medium directly implies E_{pol}, the polarization energy of the Ar medium by the Ar^+ ion core, which is not very rapidly converging with the total number of Ar considered (see discussion above in Sec. III A); this should lead to an overestimation of the binding energy in the medium and thus also influence the above comparison. In contrast, the change of the energy of the 5*s* orbital with respect to an unpolarized Ar medium ($E_{4s}^{\mathrm{crystal}} - E_{\mathrm{pol}}$), i.e., the change of the energy of the 5*s* absorption line according to Eq. (3), is equal to 0.23 eV in bulk Ar, much smaller than the corresponding value for the 4*s* orbital (0.91 eV, see Fig. 1). Incidentally, if the energy shift of the 5*s* orbital were as large as that of the 4*s* orbital, the 5*s* would be above vacuum in the present calculation and the $Ar^*(2p_{3/2}^{-1}\,5s)$ atom inside the 381 Ar atom crystal could decay by electron emission into vacuum, leaving a finite size Ar crystal polarized by the Ar^+ ion core.

Let us now consider the $Ar^*(2p_{3/2}^{-1}\,4p)$ excited state. In the bulk environment of O_h symmetry, the *p* orbital of the free atom becomes an F_{1u} orbital and remains triply degenerate.[26] Figure 8 presents a cut of the 4*p* orbital wave function for an $Ar^*(2p_{3/2}^{-1}\,4p)$ atom embedded inside bulk Ar. The plane of the cut is the same as in Fig. 6, as well as the finite size of the Ar crystal (381 atoms). The *p* orbital is polarized along the *z* axis and the other two degenerate orbitals could be defined similarly along the other two axes of the cubic cell of the fcc. One recognizes the global shape of a p_z orbital along the *z* axis, centered on the Ar^* center. The structures associated with the nearest neighbors are very strongly marked, whereas those for more distant Ar centers are weaker. Although more diffuse than the 4*s* orbital, the 4*p* does not spread much over the crystal and still presents the characteristics of an orbital confined by its nearest neighbors. The confinement interpretation is confirmed by the energy shift of the 4*p* orbital. The energy shift of the 4*p* orbital in bulk Ar (energy with respect to an unpolarized medium) amounts to 1.05 eV, similar to the value for the 4*s* orbital (0.91 eV). As for the binding energy of the 4*p* orbital with respect to a polarized Ar medium, its value in the bulk is smaller by a factor $(1.7)^{-2}$ than its value in the free atom, i.e., the continuous medium prediction. However, the shape of the 4*p* wave function in bulk Ar rather supports the confinement picture against the continuous medium picture in this case. The success of the continuum medium prediction could then be considered as fortuitous in this case, in view of the shape of the orbital wave function; alternatively, this can be

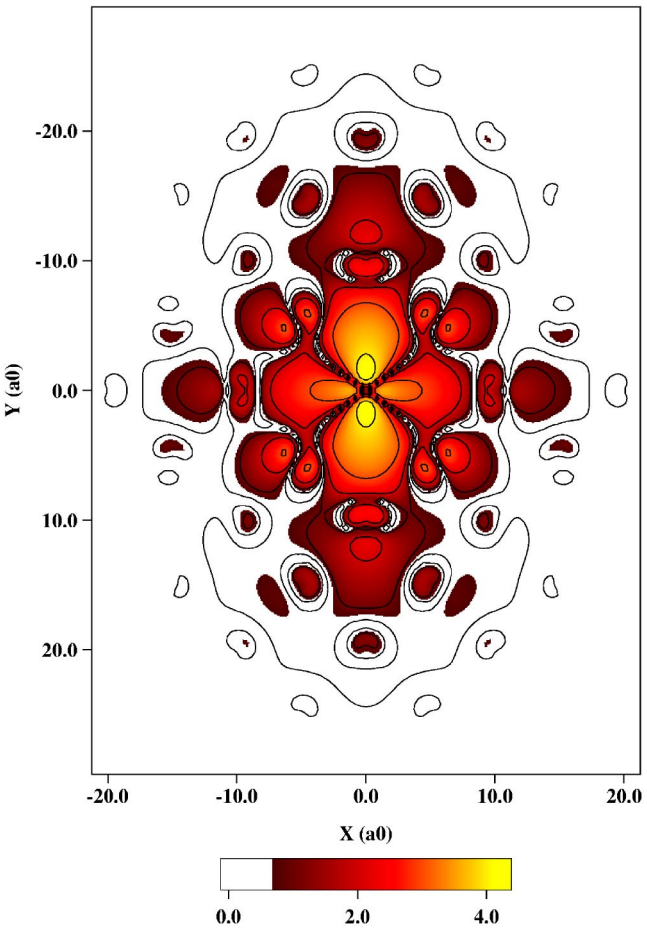

FIG. 9. (Color online) Contour plot of the resonant 3*d* orbital of a core-excited $Ar^*(2p_{3/2}{}^{-1}\ 3d)$ atom inside an fcc Ar crystal. The figure presents a cut of the logarithm of the modulus of the 3*d* electron wave function in the (100) plane (*x* and *y* coordinates). The Ar^* atom center is located at the origin of coordinates. The electron density decreases when going from yellow to orange and deep red (from light to dark gray). White corresponds to very small electron densities. The contour lines (thin full lines) correspond to 1.0 steps.

an indication of a case intermediate between discrete and continuous media interpretations.

The $Ar^*(2p_{3/2}{}^{-1}\ 3d)$ excited state inside the same bulk environment provides a case intermediate between the two situations depicted above. In the bulk environment, the *d* orbital splits into a doubly and a triply degenerate orbital.[26] Figure 9 presents a cut of the wave function of one of the 3*d* levels. The plane of the cut is the same as in Fig. 6 (*z* axis along the [100] direction and plotted as the ordinate axis) and the orbital derives from a d_z orbital. One recognizes a much distorted d_z wave. The structures around the Ar neighbors exhibit a twisted double lobe structure. The energy shift of this 3*d* orbital in bulk Ar (energy with respect to an unpolarized medium) amounts to 0.56 eV, significantly smaller than the one found for the lower lying orbitals, resulting from confinement, but larger than that for the 5*s* orbital. As for its binding energy in the Ar medium it decreases by a factor 2^2 compared to the free atom case. The behavior of this orbital can then be seen as resulting from an intermediate situation between confinement and continuous medium pictures.

D. Discussion

As discussed in Sec. II, the present results on the energy shift of the excited electron in $Ar^*(2p_{3/2}{}^{-1}\ 4s)$ yield an approximation for the total energy shift of the state and can thus be compared with the experimental determinations of the corresponding line energy in x-ray absorption spectroscopy. The experimental shift of the excitation energy of the core-excited $Ar^*(2p_{3/2}{}^{-1}\ 4s)$ state when the Ar^* is inside an Ar crystal or at its surface, compared to the excitation energy in the free atom is shown in the right panel of Fig. 1. Various experimental determinations of these two energy shifts are available.[3–7,10,11]

Let us first examine the case of bulk Ar. Experimental data spread between 0.71 and 1 eV (see right panel of Fig. 1). They were obtained from experiments either on very thick layers adsorbed on a substrate[3–7] or from the extrapolation of a series of clusters of increasing size.[10,11] Taking into account the scatter of the experimental data, the agreement with the present bulk result, 0.91 eV, is quite satisfying.

The discussion of the case where the Ar^* atom belongs to the surface of a piece of solid Ar is more difficult. Indeed, the present theoretical result depends on the surface that is considered and mainly on the number of nearest neighbors and the question arises of the number of first neighbors for a surface atom. This question has been discussed in the context of Ar clusters. Depending on the number of Ar atoms, the minimum energy structure of an Ar_N cluster changes from polyicosahedral at low *N* to bulklike fcc or hcp at large *N*.[27–30] The growth mode of the cluster, i.e., its mode of preparation can also influence the cluster structure which can be different from the minimum energy structure and should favor structures with defects.[29,30] In addition, defects or sites with a low number of first neighbors could be associated locally with an Ar-Ar distance different from that in the bulk, leading to changes in the energy shift (see Fig. 4). Björneholm *et al.*[10] interpreted the variation of the experimental $2p_{3/2}$ binding energy in surface sites on Ar clusters as due to the variation of the effective number of first neighbors in a surface site with the size of the clusters. In their modeling, the number of first neighbors varies from 5 to 8 with the size of the cluster. A similar effect should be present for a thick Ar layer, which could exhibit defects and does not form a perfect (111) plane as for 1 ML adsorption on a simple metal (see, e.g., Refs. 31 and 18). For all these reasons, it is very difficult to decide what should be the crystal structure surrounding an Ar atom when this atom is belonging to the surface of a piece of Ar crystal. Nevertheless, one can notice that the experimental data for the surface energy shift spread between 0.31 and 0.5 eV (see right panel of Fig. 1). If we assume that a number of 6 to 9 is a reasonable estimate for the number of first neighbors on the Ar surface, the theoretical predictions spread between 0.33 and 0.49 eV.

IV. CONCLUDING SUMMARY

Results of a theoretical study of the $Ar^*(2p_{3/2}{}^{-1}\ 4s)$ core-excited state inside a solid Ar environment have been pre-

sented. To analyze the role of the various neighbors in the perturbation of the excited state, a set of calculations were performed considering Ar^* surrounded by various finite size pieces of an Ar fcc crystal. The following are the main results.

The energy shift of the 4*s* excited electron compared to the free atom case is mainly dependent on the number of first neighbors. Higher order neighbors are much less perturbing.

The energy shift of the 4*s* excited electron compared to the free atom case roughly varies linearly with the number of first neighbors.

The present results reproduce the experimentally observed shift of the absorption line of the $Ar^*(2p_{3/2}{}^{-1}\,4s)$ state between the cases of a free atom, of an atom in bulk Ar and an atom belonging to the surface of solid Ar.

Different excited orbitals in the $Ar^*(2p_{3/2}{}^{-1}\,nl)$ core-excited states are differently influenced by Ar neighbors. Depending on the relative value of the orbital radius and of the nearest neighbor distance in the solid, different qualitative pictures emerge. The 4*s* orbital can be seen as confined by the nearest Ar neighbors, whereas the more diffuse 5*s* orbital is better described as an orbital expanding in a continuous dielectric medium. One thus meets the limit between a discrete microscopic description and a continuous dielectric medium description for the qualitative discussion of the behavior of low-energy electrons in the Ar solid.

ACKNOWLEDGMENT

Very efficient help from A. G. Borisov in the early stages of this work and in particular in setting up the WPP code is gratefully acknowledged.

[1] R. E. Palmer, Prog. Surf. Sci. **41**, 51 (1992).
[2] L. Sanche, J. Phys. B **23**, 1597 (1990).
[3] R. Haensel, N. Kosuch, U. Nielsen, U. Rössler, and B. Sonntag, Phys. Rev. B **7**, 1577 (1973).
[4] G. Rocker, P. Feulner, R. Scheuerer, L. Zhu, and D. Menzel, Phys. Scr. **41**, 11014 (1990).
[5] W. Wurth, G. Rocker, P. Feulner, R. Scheuerer, L. Zhu, and D. Menzel, Phys. Rev. B **47**, 6697 (1993).
[6] E. Rühl, C. Heinzel, A. P. Hitchcock, and H. Baumgärtel, J. Chem. Phys. **98**, 2653 (1993).
[7] W. Wurth and D. Menzel, Chem. Phys. **251**, 141 (2000).
[8] G. C. King, M. Tronc, F. H. Read, and R. C. Bradford, J. Phys. B **10**, 2479 (1977).
[9] L. Avaldi, G. Dawber, R. Camilloni, G. C. King, M. Roper, M. R. F. Siggel, G. Stefani, and M. Zitnik, J. Phys. B **27**, 3953 (1994).
[10] O. Björneholm, F. Federmann, F. Fössing, and T. Möller, Phys. Rev. Lett. **74**, 3017 (1995).
[11] M. Tchaplyguine, R. Feifel, R. R. T. Marinho, M. Gisselbrecht, S. L. Sorensen, A. Naves de Brito, N. Mårtensson, S. Svensson, and O. Björneholm, Chem. Phys. **289**, 3 (2003).
[12] C. Keller, M. Stichler, G. Comelli, F. Esch, S. Lizzit, W. Wurth, and D. Menzel, Phys. Rev. Lett. **80**, 1774 (1998).
[13] A. Sandell, P. A. Brühwiler, A. Nilsson, P. Bennich, P. Rudolf, and N. Mårtensson, Surf. Sci. **429**, 309 (1999).
[14] A. Föhlisch, D. Menzel, P. Feulner, M. Ecker, R. Weimar, K. L. Kostov, G. Tyuliev, S. Lizzit, R. Larciprete, F. Hennies, and W. Wurth, Chem. Phys. **289**, 107 (2002).
[15] A. Pavlychev, E. V. Semenova, A. P. Hitchcock, and E. Rühl, Physica B **208-09**, 187 (1995).
[16] V. K. Dolmatov, A. S. Baltenko, J.-P. Connerade, and S. T. Manson, Radiat. Phys. Chem. **70**, 417 (2004).
[17] D. C. Marinica, C. Ramseyer, A. G. Borisov, D. Teillet-Billy, J. P. Gauyacq, W. Berthold, P. Feulner, and U. Höfer, Phys. Rev. Lett. **89**, 046802 (2002).
[18] D. C. Marinica, C. Ramseyer, A. G. Borisov, D. Teillet-Billy, and J. P. Gauyacq, Surf. Sci. **540**, 457 (2003).
[19] J. P. Gauyacq and A. G. Borisov, Phys. Rev. B **69**, 235408 (2004).
[20] A. G. Borisov, A. K. Kazansky, and J. P. Gauyacq, Phys. Rev. B **59**, 10 935 (1999).
[21] N. W. Ashcroft and N. D. Mermin, *Solid State Physics* (Saunders College Publishing, Philadelphia, 1976).
[22] L. Kleinman and D. M. Bylander, Phys. Rev. Lett. **48**, 1425 (1982).
[23] M. D. Fleit and J. A. Fleck, J. Chem. Phys. **78**, 301 (1983).
[24] R. Kosloff, J. Phys. Chem. **92**, 2087 (1988).
[25] O. Björneholm, F. Federmann, F. Fössing, T. Möller, and P. Stampfli, J. Chem. Phys. **104**, 1846 (1996).
[26] G. Herzberg, *Molecular Spectra and Molecular Structure, III* (Van Nostrand Reinhold, New York, 1966).
[27] J. Farges, M. F. de Feraudy, B. Raoult, and G. Torchet, J. Chem. Phys. **78**, 5067 (1983).
[28] J. Farges, M. F. de Feraudy, B. Raoult, and G. Torchet, J. Chem. Phys. **84**, 3491 (1986).
[29] B. W. van de Waal, J. Chem. Phys. **98**, 4909 (1993).
[30] B. W. van de Waal, G. Torchet, and M.-F. de Feraudy, Chem. Phys. Lett. **331**, 57 (2000).
[31] K. Horn, C. Mariani, and L. Cramer, Surf. Sci. **117**, 376 (1982).